



HAL
open science

Design of Potassium-Selective Mixed Ion/Electron Conducting Polymers

Ariana Villarroel Marquez, Gerardo Salinas, Myriam Abarkan, Maël Idir,
Cyril Brochon, Georges Hadziioannou, Matthieu Raoux, Alexander Kuhn,
Jochen Lang, Eric Cloutet

► **To cite this version:**

Ariana Villarroel Marquez, Gerardo Salinas, Myriam Abarkan, Maël Idir, Cyril Brochon, et al.. Design of Potassium-Selective Mixed Ion/Electron Conducting Polymers. *Macromolecular Rapid Communications*, In press, 10.1002/marc.202070030 . hal-02564999

HAL Id: hal-02564999

<https://hal.science/hal-02564999>

Submitted on 6 May 2020

HAL is a multi-disciplinary open access archive for the deposit and dissemination of scientific research documents, whether they are published or not. The documents may come from teaching and research institutions in France or abroad, or from public or private research centers.

L'archive ouverte pluridisciplinaire **HAL**, est destinée au dépôt et à la diffusion de documents scientifiques de niveau recherche, publiés ou non, émanant des établissements d'enseignement et de recherche français ou étrangers, des laboratoires publics ou privés.

Design of potassium selective mixed ion/electron conducting polymers

*Ariana Villarroel Marquez, Gerardo Salinas, Myriam Abarkan, Maël Idir, Cyril Brochon, Georges Hadziioannou, Matthieu Raoux, Alexander Kuhn, Jochen Lang, Eric Cloutet**

Dr. A. Villarroel Marquez, Maël Idir, Dr. Cyril Brochon, Prof. Georges Hadziioannou, Dr. Eric Cloutet
Univ. Bordeaux, CNRS, Bordeaux INP, LCPO, UMR 5629, F-33615, Pessac, France
E-mail: cloutet@u-bordeaux.fr

Dr. A. Villarroel Marquez, Myriam Abarkan, Dr. Matthieu Raoux, Prof. Jochen Lang
Univ. Bordeaux, CNRS, Bordeaux INP, CBMN, UMR 5248, F-33600, Pessac, France.

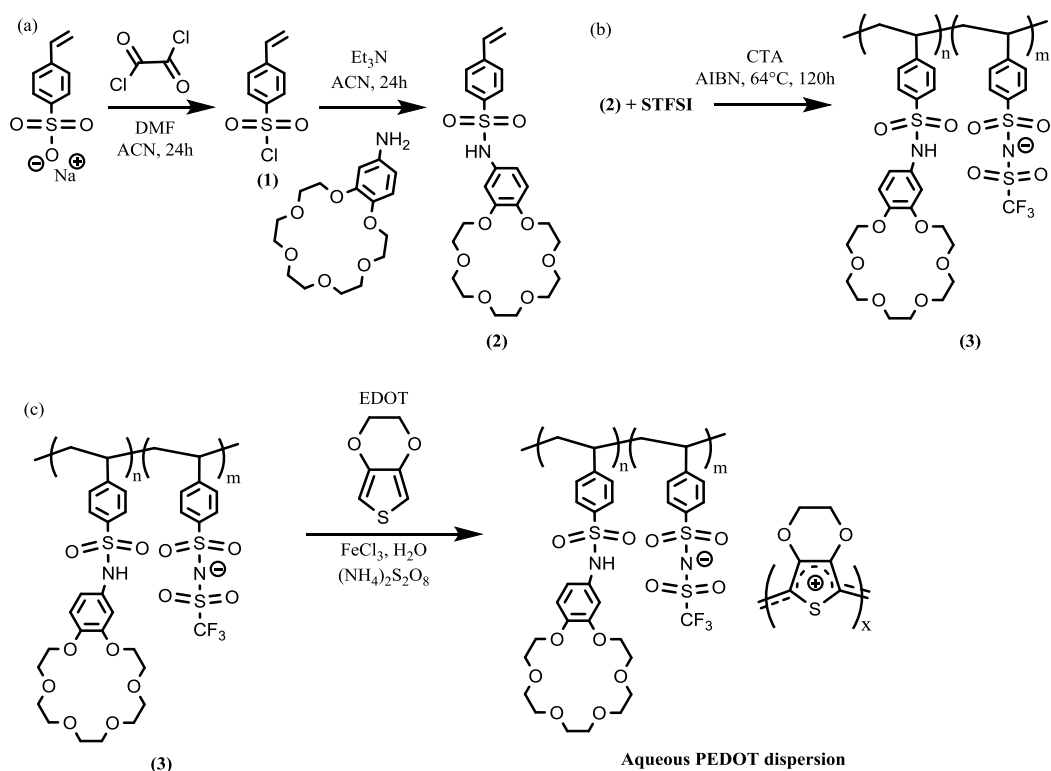
Dr. G. Salinas, Prof. A. Kuhn
Univ. Bordeaux, CNRS, Bordeaux INP, ISM, UMR 5255, F-33607 Pessac, France.

Keywords: Mixed conducting polymers, PEDOT, crown-ether, ion sensing, coulombometry.

An approach providing cation selective PEDOT:polyelectrolyte mixed conductors is presented in this communication, based on the structural modification of this ambivalent (ionic and electronic conductive) polymer complex. First, an 18-crown-6 moiety was integrated into the styrene sulfonate monomer structure as a specific metal cation scavenger particularly targeting K^+ vs Na^+ detection. This newly functionalized monomer has been characterized by 1H - NMR titration to evaluate the ion selectivity. Aqueous PEDOT dispersion inks containing the polymeric ion-selective moieties have been designed and their electrical and electrochemical properties have been analysed. These biocompatible inks are the first proof-of-concept step towards ion selectivity in view of their interfacing with biological cells and microorgans of interest in the field of biosensors and physiology.

1 Mixed conducting polymer films are materials that have gained considerable interest, due to
2 the synergy between the polyelectrolyte, for ionic transport, and the conjugated conducting
3 polymer, for electronic transport.^[1-2] Poly-(3,4-ethylenedioxythiophene) (PEDOT),^[3]
4 stabilized by poly(styrene sulfonate) (PSS), is one of the most used mixed conducting
5 polymer system for the development of organic electronics.^[4-6] PSS has a double role in the
6 blend; it works as the counter ion for the conducting doped PEDOT chains and stabilizes the
7 insoluble charged PEDOT in aqueous suspensions. PEDOT:PSS dispersions have been used
8 to obtain thin film electrodes for different applications such as solar cells (OPV),
9 electrochromic electrodes, flexible screen devices (OLED) and organic electrochemical
10 transistors (OECTs).^{[4],[7-8]} In the latter, since mixed conduction occurs in the volume of these
11 devices, the low current resistance of the films allows better electrical recordings with local
12 signal amplification and consequently unprecedented signal detection in biology
13 applications^[9-10] pH^[11] and ion monitoring.^[12-13] An interesting alternative is the enhancement
14 of ion selectivity of these materials by tuning the chemical structures of the conducting
15 polymer or the polyelectrolyte, in order to target an analyte of interest.^[14] Complex
16 functionalized polythiophenes, with selective moieties targeting anion and cation analysis
17 have been synthesized.^[15-16] Although these mixed conducting polymers present high
18 selectivity, the poor solubility of the monomer in water imposes the use of organic solvents
19 during the electropolymerization. In the frame of a more environmental friendly approach, a
20 promising method to improve solubility may be provided by functionalization of the water
21 soluble polyelectrolyte. In this work, we present an approach to confer cation selectivity to a
22 PEDOT:polyelectrolyte mixed conductor. A specific metal cation scavenger particularly
23 targeting K^+ detection, the 18-crown-6 moiety, was integrated into the styrene sulfonate
24 monomer through the modification of the corresponding anion. The 18-crown-6 moiety has
25 been chosen due to its well-known affinity towards the target cation K^+ , based on its size
26 matching, as well as for the commercial availability of its functional derivatives (*i.e.*

1 aminocrown).^[17] Potassium (K^+) was selected as a monovalent target among all the possible
 2 choices, due to its importance in the generation and dissipation of electrical cell signals as
 3 changes in K^+ efflux from cells play a major role in cell depolarization and repolarization of
 4 membrane potentials.^[18] Incorporation of the ionophore 15-crown-5 in electrodeposited
 5 PEDOT for monovalent cations analysis has been previously reported.^[19] However, the
 6 electrodeposition requires the presence of different counter ions (PSS, chloride and
 7 perchlorate) to keep the electroneutrality of the charged PEDOT chains.

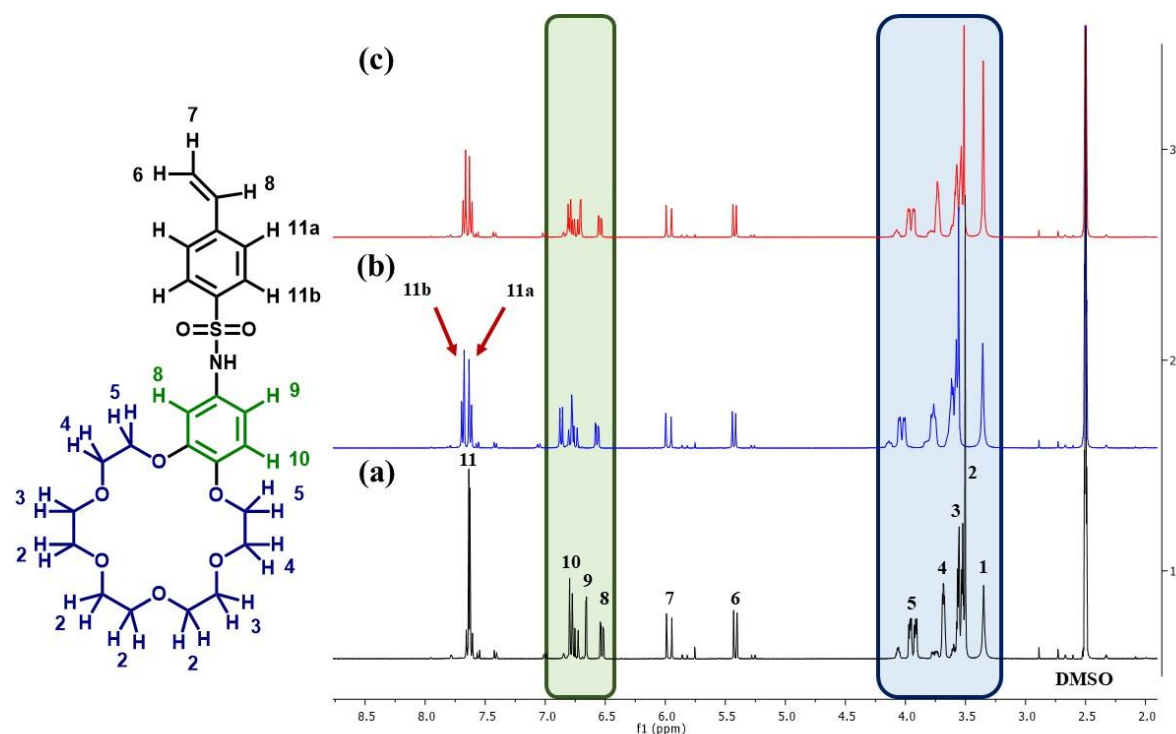


8
 9 **Scheme 1.** (a) Synthetic route to obtain the 4-styrenesulfonyl(phenyl-18-crown-6) imide
 10 monomer (2); (b) RAFT copolymerization of PEDOT counterpart (3) in the presence of CTA:
 11 Chain transfer agent 2-(Dodecylthiocarbonothioylthio)-2-methylpropionic acid, AIBN:
 12 Initiator 2,2'-Azobis(2-methylpropionitrile) with m: fraction of 4-styrenesulfonyl
 13 (trifluoromethylsulfonyl) imide (STFSI) and n: fraction of monomer (2). (c) Synthesis of ion-
 14 sensitive aqueous PEDOT dispersion by oxidative polymerization of EDOT in water in the
 15 presence of FeCl_3 and $(\text{NH}_4)_2\text{S}_2\text{O}_8$.

1 Synthesis of the newly functionalized monomer (2) was confirmed by $^1\text{H-NMR}$, $^{13}\text{C-NMR}$
2 and EIS-HRMS spectroscopy (see supporting information, monomer synthesis and
3 spectroscopy characterization). This functionalized monomer (2) was characterized by $^1\text{H-}$
4 NMR titration to evaluate its ion selectivity (*i.e.* K^+ vs Na^+). Aqueous PEDOT dispersion inks
5 containing the ion-selective moieties were then designed and their electrical and
6 electrochemical properties have been analyzed. Synthesis of the ion selective monomer,
7 copolymerization of the polyelectrolyte and synthesis of the conductive inks are illustrated in
8 Scheme 1. First, the synthesis of (2) has been achieved in a two-step reaction path. The
9 formation of the styrenesulfonyl chloride (1) was followed by reaction with the functionalized
10 amino phenyl-18-crown-6, to obtain the targeted monomer (2). The $^1\text{H-NMR}$ spectrum of (2)
11 (Figure SI-1) shows the corresponding signals for the styrene aromatic protons at 7.4 ppm and
12 7.7 ppm. Vinyl protons are evidenced by the presence of the signals at 5.37 ppm and 5.82
13 ppm. The signal of $-\text{CH}_2\text{-O-}$ from the crown moiety is assigned at 3.75 ppm. Finally, the
14 multiplet signal at 6.62 ppm corresponds to the aromatic protons of the crown moiety. The
15 corresponding $^{13}\text{C-NMR}$ spectrum of (2) also confirms the expected monomer structure
16 (Figure SI-2).

17 Ion selectivity toward K^+ vs. Na^+ of newly designed monomer (2) was first investigated via
18 $^1\text{H-NMR}$ titration at various concentrations of potassium and sodium perchlorate (Figure SI-3
19 and Figure SI-4). Figure 1 shows for instance the chemical shifts obtained during the NMR
20 study of monomer (2) in the presence of 2 molar equivalents in concentration of potassium
21 and sodium perchlorate, respectively. Thus, in the presence of K^+ , the signals related to the
22 protons in the proximity of the crown ether cavity (signals 9-10 and 2-5) are shifted, as
23 compared to the $^1\text{H-NMR}$ spectrum of the pristine monomer (Figure 1b vs. 1a) in the absence
24 of K^+ . This behavior can be attributed to the formation of a coordination compound between
25 the K^+ and the crown ether moiety (signals 2-3 in Fig 1b vs 1a). Furthermore, the chemical
26 shifts related to the vinyl protons (signals 6-7) were not affected by the presence of the cation.

1 This confirms that the binding interaction with the monovalent cations occurs as expected
2 through the crown ether moiety. However, when $^1\text{H-NMR}$ study was performed in the
3 presence of sodium perchlorate at the same concentration as K^+ , the variation of the chemical
4 shift was negligible (signals 2-3 in Figure 1c vs 1a). From the analysis of the chemical shift as
5 a function of the salt concentration the binding isotherms were obtained (Figure SI-5). Using a
6 1:1 binding model of the experimental data, the association constants (k_a) of (2) with both
7 cations were evaluated ($k_{a, \text{Na}} = 121.7 \pm 6.9 \text{ M}^{-1}$ and $k_{a, \text{K}} = 1026.2 \pm 118.3 \text{ M}^{-1}$). As the K_a is
8 one order of magnitude higher for potassium in comparison to sodium, these results confirm
9 the high selectivity of (2) for the K^+ cation in accordance with the crown ether size-matching
10 rule. In addition, from the dissociation constants ($k_d = 1/k_a$), a stronger binding of K^+ in this
11 solvent can be inferred. Finally, saturation of the binding sites was obtained only by the
12 addition of the potassium salt (plateau range in figure SI- 5).



13
14 **Figure 1.** $^1\text{H-NMR}$ Spectra (DMSO- d_6 , 400 MHz) obtained for monomer (2) in the absence
15 (a) and in the presence of 2 molar equivalents of (b) potassium perchlorate and (c) sodium
16 perchlorate.

1 Monomer (2) was then integrated into a polyanion through copolymerization with the
2 monomer 4-styrenesulfonyl (trifluoromethylsulfonyl) imide (STFSI). PSTFSI derivative has
3 been reported by us as an alternative to PSS in PEDOT:PSS materials for further use in
4 transparent organic electrodes.^{[8],[20]} The STFSI fraction provides solubility in water, whilst
5 the functionalized monomer (2) confers the ion-sensitive ability. It appears that the dispersity
6 gets larger as the content in monomer (2) is increased, *i.e.* from 5 to 15% (Table 1) due to the
7 statistical distribution of these moieties in the different polymer chains. Moreover, when the
8 content of the monomer (2) increases up to 40% or 50%, it became complicated to reach the
9 targeted chain length (M_w) (Table 1). A copolymer at a ratio of 85 wt. % of STFSI and 15
10 wt. % of monomer (2) has been taken as a case study from a larger copolymer family (Table
11 1). A polyanion P(STFSI-*co*-S(18-crown-6)) (3) with an apparent molar mass of 135 kDa,
12 was for instance obtained (Figure SI-6, PS standard calibration and DMF solvent) with quite
13 broad distribution which can be attributed to specific interactions with SEC columns. The ¹H-
14 NMR of the P(STFSI-*co*-S(18-crown-6)) (Figure SI-7) clearly shows broadening of signals as
15 compared to the initial monomers' spectra in accordance with the expected expansion of
16 polymer signals in this type of high molar masses polyelectrolytes.^[21] The presented
17 copolymer ratio is the theoretical weight percentage (wt%) ratio between STFSI and
18 monomer (2) used for the polymer synthesis. Experimentally it is not possible to quantify the
19 copolymer ratio by the NMR spectra, as the initiator signal overlaps in the aliphatic region
20 with the signals related to the alkyl polymer backbone ($\delta = 0.75$ - 2.25 ppm). However, the ¹H-
21 NMR chemical shifts from the aromatic rings, polystyrene backbone and crown ether moieties
22 could be assigned at $\delta = 6.59$ - 7.54 ppm, $\delta = 1.44$ ppm and $\delta = 3.53$ - 4 ppm respectively and thus
23 confirmed the copolymer synthesis and correlates with the ratio between comonomers.²¹

24

25 **Table 1.** Summary of polyanion (3) synthesized, and used for the stabilization of ion-sensitive
26 PEDOT dispersions. M_0 : STFSI monomer; M : functionalized monomer (2); n_{M_0} / n_M : molar

1 ratio between both monomers; M_w : Average of the apparent molecular mass (kDa) of the
 2 obtained polyanions copolymers^{a)} and \mathcal{D} : Dispersity as obtained from SEC^{a)} analysis in DMF
 3 using PS standard calibration

Theoretical polyelectrolyte composition [M ^o _{WT%} -M _{WT%}]	n_{m0}/n_M	M_w [kDa] ^{a)}	\mathcal{D} ^{a)}
PSS ₉₅ -PS18cr6 ₅	13.6	112	1.3
PSTFSI ₉₀ -PS18cr6 ₁₀	6.5	127	2.3
PSTFSI ₈₅ -PS18cr6 ₁₅	4.1	135	2.6
PSTFSI ₈₅ -PS18cr6 ₁₅ (250kDa)	4.1	208	2.8
PSTFSI ₇₀ -PS18cr6 ₃₀	1.7	144	2.3
PSTFSI ₆₀ -PS18cr6 ₄₀	1.1	44	1.4
PSTFSI ₅₀ -PS18cr6 ₅₀	0.7	96	2.3

4
 5 The ion-sensitive functionalized polyelectrolyte, P(STFSI-co-S(18-crown-6)), was
 6 subsequently used as a stabilizer/counterpart of aqueous PEDOT dispersions during the
 7 oxidative *in-situ* polymerization of EDOT^[21] in the presence of iron chloride and ammonium
 8 persulfate; see Scheme 1c). PEDOT inks were obtained after polymerization for 64h at 10°C
 9 under inert atmosphere, then recovered through purification via ultrafiltration. As illustrative
 10 example, an initial copolymer solution (Figure SI-8a) is presented, acting as stabilizer of
 11 PEDOT favoring the complex formation and stability of the PEDOT dispersion in water when
 12 the polymerization takes place (Figure SI-8b).
 13 Processable and stable aqueous inks were obtained, containing the hydrophobic ion-selective
 14 moiety in the polyelectrolyte chains. However, stable PEDOT inks were difficult to obtain
 15 when trying to incorporate more than 50% (in weight content) of crown ether modified
 16 styrene subunits into the copolymer. In fact, in these cases the dispersion was unstable and the
 17 polymer precipitated. Spin-coated PEDOT films presented conductivities in the mS cm⁻¹
 18 range ($\sigma < 1366$ mS cm⁻¹). Although this is less than what is observed for PEDOT:PSS and
 19 PEDOT:PSTFSI (190 S cm⁻¹ and 110 S cm⁻¹ respectively), this conductivity range is
 20 sufficient for bioelectronics applications.

1 In order to evaluate the electrochemical properties of the films and provide more evidence for
2 the occurrence of ion selectivity of these mixed conducting polymers, *in-situ* electrochemical
3 conductance experiments were carried out.^[22] The electrochemical characterization of drop
4 casted films was evaluated in an aqueous 0.1 M tetramethyl ammonium chloride (TMAC)
5 solution (Figure 2a and b). Two separate IDME electrodes, covered with the same conductive
6 ink, were used to analyze their electrochemical response in the presence of potassium and
7 sodium respectively (Figure 2a and b). Since during drop casting, the thickness control of the
8 films is limited, normalized currents are presented in order to allow a reasonable comparison
9 of the samples.

10 Initially, during the first potential sweep, peaks of current were not observed for both films
11 (Fig. 2 (a) and (b)). Subsequently, a peak of current starts to appear, between 0.36 V and 0.38
12 V vs Ag^o. This additional anodic reaction is attributed to the oxidation of the aniline moiety
13 attached to the crown ether group along the P(STFSI-*co*-S(18-crown-6)) polyanion. The
14 absence of this oxidation peak, at the first potentiodynamic scan, is due to the low current
15 attributed to such redox process, which overlaps with the oxidation current of the different
16 oligomeric PEDOT chains. It should be noted that PEDOT:PSS and PEDOT:PSTFSI do not
17 show any anodic peak in this range of potentials (Figure SI-9a and b). The conductance
18 profile of the films shows a quasi-linear increase during the potential sweep, caused by the
19 formation of mobile charges in the PEDOT backbone. Whereas, a gradual decrease of
20 conductance was observed as the cycling proceeds (from 5.44 ± 0.75 mS to 4.61 ± 0.37 mS)
21 (Figure SI-10a and b). This decrease is attributed to a conformational rearrangement of the
22 oligomeric chains of the polymer blend and not to a limitation of charge hopping caused by
23 the trapped positive charges formed during the aniline oxidation.^[23] In order to provide more
24 evidence of these conformational changes, the charge-potential plots were obtained by
25 integration of the potentiodynamic plots.^[24] From the coulometric response it is
26 possible to identify changes in structural components driven by electrochemical reactions

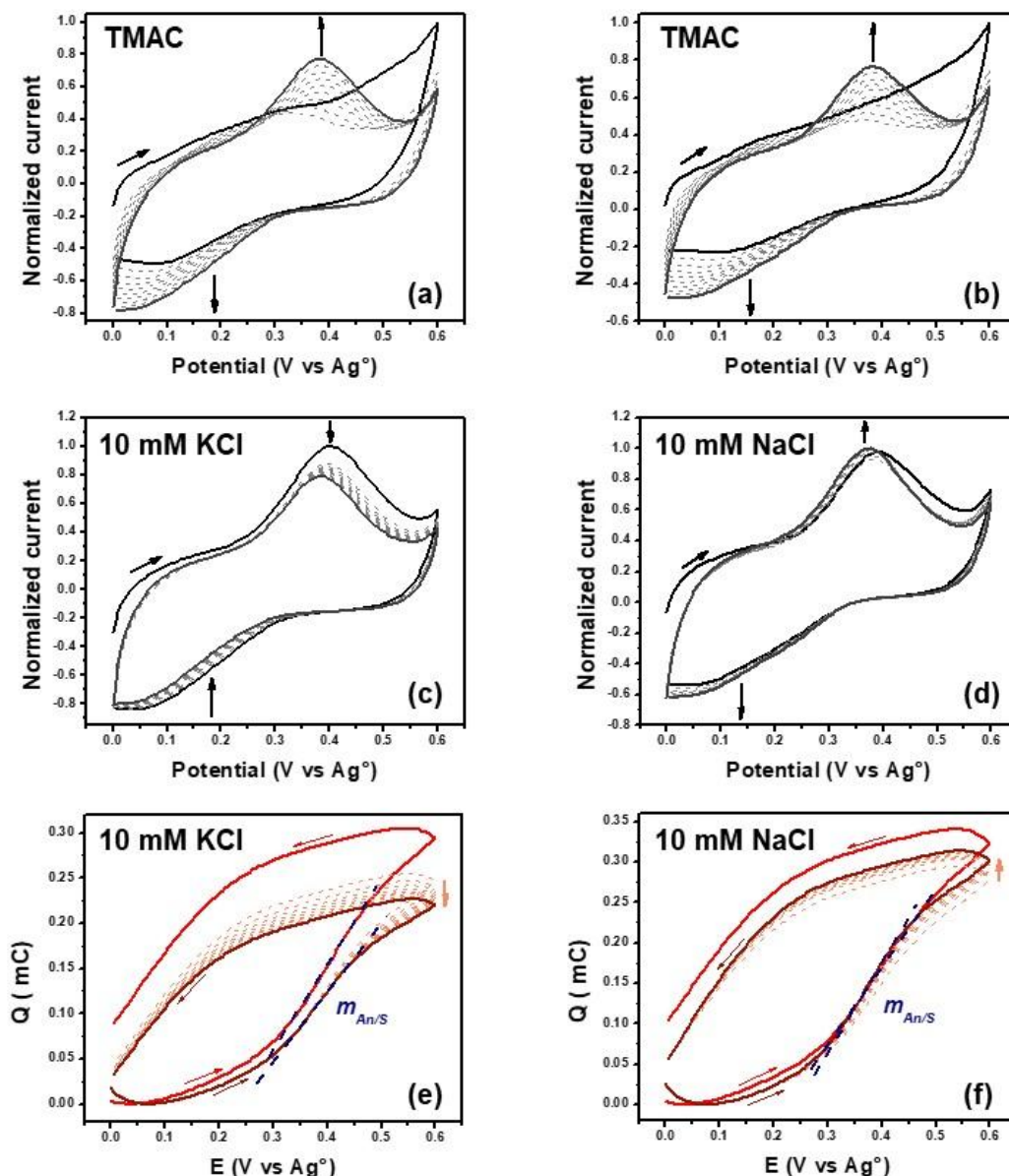
1 inside the conducting polymer matrix.^[25-28] These charge-potential plots have been used by
2 Otero *et al.*, by means of the electrochemically stimulated conformational relaxation model
3 (ESCR) to explain the reversible and irreversible structural changes driven by electrochemical
4 reactions of conducting polymers exchanging cations.^[29] Since, for mixed conducting
5 materials, composed of conducting polymers and anionic polyelectrolytes, the anion remains
6 inserted in the conducting polymer matrix during the charge/discharge process, exchange of
7 cations occurs. According to the ESCR model, variations in the slope values of the charge-
8 potential plots are attributed to conformational changes of the polymer matrix.^[24]

9 The coullovoltammetric response of the films, in a 0.1 M TMAC aqueous solution (Figure SI-
10 11a), presents in the first cycle, starting from the minimum of charge, two oxidation
11 processes: an oxidation/shrinking ($m_{O/S} = 0.48 \text{ mC V}^{-1}$) and an oxidation/compaction^[30] ($m_{O/C}$
12 $= 0.78 \text{ mC V}^{-1}$), both caused by the release of cations from the polymer matrix. The latter is
13 followed, at the beginning of the cathodic sweep, by some oxidation inertia and two reduction
14 processes: a reduction/relaxation ($m_{R/R} = 0.16 \text{ mC V}^{-1}$) and a reduction/swelling ($m_{R/S} = 0.50$
15 mC V^{-1}), caused by the insertion of tetramethyl ammonium cations. During subsequent scans,
16 the slope value of the oxidation/shrinking and the oxidation/compaction slope decreases
17 (Figure SI-11b, $m_{O/S} = 0.26 \text{ mC V}^{-1}$, $m_{O/C} = 0.46 \text{ mC V}^{-1}$), whilst a new oxidation process
18 appears, between 0.30 V and 0.45 V vs Ag° , with a concomitant increase of slope ($m_{An/S} =$
19 0.81 mC V^{-1}). Due to the range of potential where it appears, this is attributed to the positive
20 charge formed during the aniline oxidation^[31] that, in addition to the oxidation of PEDOT,
21 causes a faster oxidation/shrinking process, hereafter referred to as aniline-
22 oxidation/shrinking. Finally, during the cathodic sweep, a faster reduction/swelling process
23 was observed ($m_{R/S} = 0.77 \text{ mC V}^{-1}$). This may be attributed to a positive “charge trapping”,
24 which requires a faster exchange of cations and anions inside the polymer matrix to keep
25 electroneutrality.

1 The ion selectivity was evaluated in a 0.1 M TMAC aqueous solution in the presence of 10
2 mM potassium or sodium chloride (Figure 2c and d, respectively). In the presence of KCl, a
3 continuous decrease in current of the aniline oxidation peak (20.5 %) was observed. In
4 contrast, in the NaCl solution, first a small decrease of the aniline oxidation peak was
5 obtained, followed by a slow increase of the peak current (2.4 %). A possible explanation for
6 this observation is that potassium ions provide an electron withdrawing effect on the aniline
7 moiety, which causes an anodic shift of the oxidation potential of the aniline. Thus, the
8 amount of aniline present and able to get oxidized at 0.38 V vs Ag^o decreases as the cycling
9 proceeds. The absence of an oxidation peak for the new K⁺-aniline complex, is due to the low
10 current attributed to such a redox process, which may overlap with the oxidation current of
11 the different oligomeric PEDOT chains as it was stated previously. In the presence of sodium,
12 the cation does not fit into the crown ether cavity and it is easier to oxidize the aniline moiety.
13 Finally, for both cations, the conductance profile of the films shows the same quasi-linear
14 variation during the potential sweep, whereas a small decrease of conductance was observed
15 as a function of the potential scans ($\Delta G_{p-K} = 0.17 \pm 0.01$ mS and $\Delta G_{p-Na} = 0.28 \pm 0.11$ mS)
16 (Figure SI-10a and b). Thus, the charge hopping process is not influenced by the presence of
17 different cations.^[23]

18 From the charge-potential plots of the films, in the presence of KCl and NaCl (Figure 2e and f,
19 respectively), the change of the maximum oxidation charge (ΔQ) after 10 potentiodynamic
20 cycles was evaluated ($\Delta Q_{K^+} = 88.70 \pm 1.59$ μ C and $\Delta Q_{Na^+} = 48.31 \pm 5.65$ μ C). As the ΔQ for
21 potassium is the double in comparison to sodium, these results confirm the selectivity of the
22 films for the K⁺ cation in accordance with the size-matching rule. In addition, the
23 coulombometric response presents, for all the cycles, the same oxidation/reduction process
24 as in the absence of the monovalent cations (Figure 2e and f). As the experiment proceed,
25 changes on the slope for all the oxidation/reduction process can be observed. From the
26 charge-potential plots (Figure 2e and f, respectively), it can be seen a higher variation of the

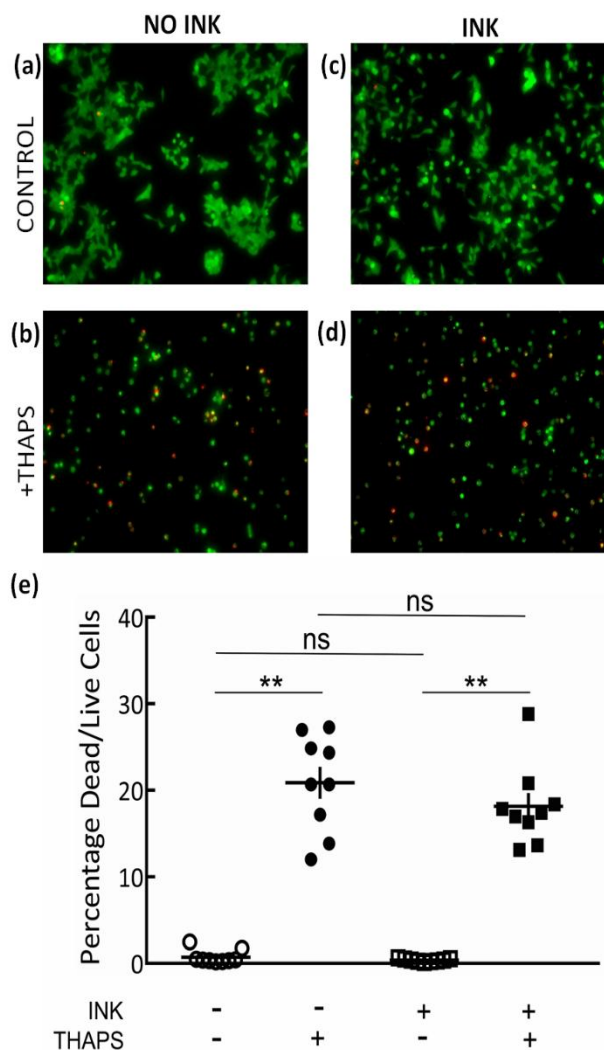
1 slope for the aniline-oxidation/shrinking and the reduction/swelling process. In the presence
2 of K^+ the aniline-oxidation/shrinking and the reduction/swelling present a decrease in the
3 slope value ($\Delta m_{An/S K} = -0.19 \text{ mC V}^{-1}$, $\Delta m_{R/S K} = -0.03 \text{ mC V}^{-1}$). However, in the NaCl solution,
4 both processes show an increase in the slope value ($\Delta m_{An/S Na} = 0.08 \text{ mC V}^{-1}$, $\Delta m_{R/S Na} = 0.10$
5 mC V^{-1}). Since potassium ions, trapped inside the crown ether cavity, are not expelled during
6 the aniline-oxidation/shrinking process, an abrupt rearrangement of the oligomeric chains
7 (between 1st and 2nd cycle) followed. This may be due to a slow mass insertion/repulsion of
8 ions during the charge/discharge process. These results correlate with the binding constants
9 obtained by ¹H-NMR ($k_{a, Na} = 121.7 \pm 6.9 \text{ M}^{-1}$ and $k_{a, K} = 1026.2 \pm 118.3 \text{ M}^{-1}$), where the
10 binding constant for potassium, suggests the formation of a K^+ -aniline complex inside the
11 polymer matrix. Such a high value of a binding constant is the first indicator of a poor release
12 of K^+ trapped in the K^+ -aniline complex.



1
 2 **Figure 2.** Potentiodynamic study of drop casted PEDOT/ P(STFSI_{85-co}-S18cr₆₁₅) films in a
 3 0.1 M TMAC aqueous solution using $E_{\lambda} = 0.6$ V vs Ag[°], 10 cycles, $\nu = 10$ mV s⁻¹ and ΔV on
 4 the WE = 10 mV, WE = Pt IDMAE, CE = Pt foil, in the absence (a and b) and in the presence
 5 of (c) 10 mM KCl and (d) 10 mM NaCl. Charge-potential plots in the presence of (e) 10 mM
 6 KCl and (f) 10 mM NaCl.
 7 Finally, in order to prepare for a future integration of these new ion-sensitive mixed
 8 conducting polymer complexes with biological systems, cell viability was evaluated on such
 9 PEDOT films. The quantification of the ratio between dead and total number of cells (dead +
 10 alive) grown on these films was comparable to the one in control conditions, suggesting an

1 unchanged growth of β cells on the coverslips covered with films (Figure 3). Thus the
2 polymer material does not exhibit a major cytotoxic effect under the conditions tested. These
3 results open up the possibility of interfacing these ion-sensitive polymers with pancreatic β -
4 cells, who play a key role in nutrient homeostasis and in diabetes.^{[18],[32]}

5 In conclusion, a new approach was presented to introduce cation selectivity in a mixed
6 conducting polymer material. A specific metal cation scavenger, particularly targeting K^+ ,
7 was integrated in the PEDOT: PSTFSI complex through the polyanion counterpart by
8 appropriate modification of the styrene subunits. We achieved synthesis and characterization
9 of a functionalized styrene derivative with an ion-selective moiety, *i.e.* 18-crown-6, monomer
10 (2). This monomer was used for the synthesis of a polyanion copolymer, which was then used
11 as a substitute to PSS in the oxidative dispersion polymerization of EDOT in water. All these
12 new compounds have been evaluated for their ability to sense K^+ metal cations. First,
13 monomer (2) showed a higher affinity for K^+ compared to Na^+ . Second, the PEDOT inks
14 composed of such polyanions displayed interesting new electrical and electrochemical
15 characteristics. By *in-situ* electrochemical conductance measurements and the correspondent
16 charge-potential plots, the higher affinity for K^+ as compared to Na^+ of these PEDOT
17 materials has been confirmed. Finally, these materials were not cytotoxic and therefore
18 qualify for applications such as recordings of K^+ -dependent electrical signals in pancreatic β -
19 or other cells via the fabrication of ion selective OECTs.



1
2 **Figure 3.** Cytotoxicity study of the ion sensitive inks: Clonal β cells (INS832-13) cultured for
3 72 h on (a, c) control coverslips or coverslips covered with the ink studied (PEDOT: PSTFSI-
4 85-co-P(2)-15 with 18-crown-6 moieties). (b, d) Apoptosis induced by thapsigargin (6h, 10
5 μ M) on control coverslips or coverslips covered with the same ink. All micrographs present
6 merged images (green: FYTC filter, live cells; red: YFP filter, dead cells). (e): quantitative
7 assessment of apoptosis. Given are individual data points, means and SEM; N= 9. **,
8 $p < 0.001$; ns, not significant (Kruskal Wallis and Dunne post-hoc test)

9 **Supporting Information**

10 Supporting Information is available from the Wiley Online Library or from the author.

11

12 **Acknowledgements**

13 We are grateful for funding from the LabEx AMADEUS-0042 with the help of the French
14 government "Initiative d'excellence" (to EC and JL), from ANR MULTISPOT ANR-17-
15 CE09-0015 (to EC, AK and JL) and the IDEX/CNRS PEPS "MULTISEPT" attributed to M.R.
16 Authors thank for help from the staff of ELORPrintTec (ANR-10-EQPX-28-01) and LCPO /
17 Arkema / ANR Industrial Chair 'HOMERIC' (ANR-13-CHIN-0002-01), as well as Eva M.
18 Muñoz from Affinimeter.

19

Received: ((will be filled in by the editorial staff))

Revised: ((will be filled in by the editorial staff))

Published online: ((will be filled in by the editorial staff))

1
2
3
4

5 References

- 6 [1] C. M. Pacheco-Moreno, M. Schreck, A. D. Scaccabarozzi, P. Bourgun, G. Wantz, M.
7 M. Stevens, O. J. Dautel, N. Stingelin, *Adv. Mater.* **2017**, *29*, 1604446.
- 8 [2] S. Inal, G. G. Malliaras, J. Rivnay, *Nat. Comm.* **2017**, *8*, 1767.
- 9 [3] L. B. Groenendaal, F. Jonas, D. Freitag, H. Pielartzik, J. R. Reynolds, *Adv. Mater.*
10 **2000**, *12*, 481.
- 11 [4] Y. Wen, J. Xu, *J. Pol. Sci. A* **2017**, *55*, 1121.
- 12 [5] M. Berggren, X. Crispin, S. Fabiano, M. P. Jonsson, D. T. Simon, E. Stavrinidou, K.
13 Tybrandt, I. Zozoulenko, *Adv. Mater.* **2019**, *31*, 1805813.
- 14 [6] H. Shi, C. Liu, Q. Jiang, J. Xu, *Adv. Electron. Mater.* **2015**, *1*, 1500017.
- 15 [7] J. H. Kim, C. W. Joo, J. Lee, Y. K. Seo, J. W. Han, J. Y. Oh, J. S. Kim, S. Yu, J. H.
16 Lee, J. I. Lee, C. Yun, B. H. Choi, Y. H. Kim, *Macro. Rapid. Comm.* **2016**, *37*, 1427.
- 17 [8] A. I. Hofmann, E. Cloutet, G. Hadziioannou, *Adv. Electron. Mater.* **2018**, *4*, 1700412.
- 18 [9] D. Khodagholy, T. Doublet, P. Quilichini, M. Gurfinkel, P. Leleux, A. Ghestem, E.
19 Ismailova, T. Hervé, S. Sanaur, C. Bernard, G. G. Malliaras, *Nat. Commun.* **2013**, *4*, 1575.
- 20 [10] P.-O. Svensson, D. Nilsson, R. Forchheimer, M. Berggren, *Appl. Phys. Lett.* **2008**, *93*,
21 203301.
- 22 [11] F. Mariani, I. Gualandi, M. Tassarolo, B. Fraboni, E. Scavetta, *ACS Appl. Mater.*
23 *Interfaces* **2018**, *93*, 203301.
- 24 [12] U. Lange, N. V. Roznyatovskaya, V. M. Mirsky, *Anal. Chim. Acta* **2008**, *614*, 1.
- 25 [13] D. T. McQuade, A. E. Pullen, T. M. Swager, *Chem. Rev.* **2000**, *100*, 2537.
- 26 [14] J. G. Ibanez, M. E. Rincon, S. Gutierrez-Granados, M. Chahma, O. A. Jaramillo-
27 Quintero, B. A. Frontana-Uribe, *Chem. Rev.* **2018**, *118*, 4731.

- 1 [15] A. Aydogan, A. Koca, M. K. Şener, J. L. Sessler, *Org. Lett.* **2014**, *16*, 3764.
- 2 [16] S. Wustoni, C. Combe, D. Ohayon, M. H. Akhtar, I. McCulloch, S. Inal, *Adv. Funct.*
3 *Mater.* **2019**, 1904403.
- 4 [17] J. M. Lehn, J. P. Sauvage, *J. Chem. Soc. D* **1971**, *9*, 440.
- 5 [18] J. Tien, D. M. Young, Y. N. Jan, L. Y. Jan, in *From Molecules to Networks*, (J. H.
6 Byrne, R. Heidelberger, M.N. Waxham), Academic Press: Boston, **2014**, p 323.
- 7 [19] M. Jeszke, K. Trzcinski, J. Karczewski, E. Luboch, *Electrochim. Acta* **2017**, *246*, 424.
- 8 [20] M. Mumtaz, K. Aissou, D. Katsigiannopoulos, C. Brochon, E. Cloutet, G.
9 Hadziioannou, *RSC Advances* **2015**, *5*, 98559
- 10 [21] A. I. Hofmann, W. T. T. Smaal, M. Mumtaz, D. Katsigiannopoulos, C. Brochon, F.
11 Schütze, O. R. Hild, E. Cloutet, G. Hadziioannou, *Angew. Chem. Int. Ed.* **2015**, *54*, 8506.
- 12 [22] G. Salinas, B. A. Frontana-Uribe, *ChemElectroChem* **2019**, *6*, 4105.
- 13 [23] H.-h. Yu, A. E. Pullen, M. G. Buschel, T. M. Swager, *Angew. Chem. Int. Ed.* **2004**, *43*,
14 3700.
- 15 [24] T. F. Otero, *Electrochim. Acta*, **2016**, *212*, 440.
- 16 [25] T. F. Otero, M. Alfaro, V. Martinez, M. A. Perez, J. G. Martinez, *Adv. Funct. Mater.*
17 **2013**, *23*, 3929.
- 18 [26] T. F. Otero, S. Beaumont, *Sensors and Actuators B*, **2017**, *253*, 958.
- 19 [27] T. F. Otero, S. Beaumont, *Electrochim. Acta*, **2017**, *258*, 1293.
- 20 [28] T. F. Otero, S. Beaumont, *Electrochim. Acta*, **2017**, *257*, 403.
- 21 [29] T. F. Otero, L. Valero, J. G. Martinez, *Electrochim. Acta*, **2017**, *246*, 89.
- 22 [30] According to the ESCR model an oxidation/shrinking process is associated to the p-
23 doping of PEDOT with the expulsion of cations and solvent, whilst an oxidation/compaction
24 is associated to the conformational movements of the chains in order to occupy the
25 unoccupied volume left by the cations and solvent molecules.
- 26 [31] G. Ćirić-Marjanović, *Synth. Met.* **2013**, *177*, 1.

- 1 [32] D. A. Koutsouras, R. Perrier, A. Villarroel Marquez, A. Pirog, E. Pedraza, E. Cloutet,
- 2 S. Renaud, M. Raoux, G. G. Malliaras, J. Lang, *J. Mat. Sci & Eng. C* **2017**, *81*, 84.
- 3

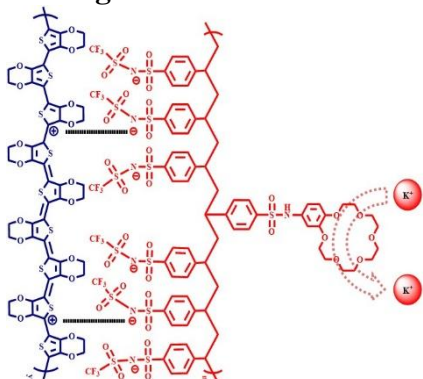
1 **ToC text:** Differentiating and sensing K^+ cations vs Na^+ through specific functionalization of
2 mixed conducting PEDOT complexes

3
4 **Keywords** Mixed conducting polymers, PEDOT, crown-ether, ion sensing, coul voltammetry

5
6 **C. Author 2, D. E. F. Author 3, A. B. Corresponding Author*** Ariana Villarroel Marquez,
7 Gerardo Salinas, Myriam Abarkan, Maël Idir, Cyril Brochon, Georges Hadziioannou,
8 Matthieu Raoux, Alexander Kuhn, Jochen Lang, Eric Cloutet*

9
10 **Title** Design of potassium selective mixed ion/electron conducting polymers

11
12 **ToC figure**



13
14
15
16

1
2 Copyright WILEY-VCH Verlag GmbH & Co. KGaA, 69469 Weinheim, Germany, 2018.

3
4 **Supporting Information**

5
6 **Design of potassium selective mixed ion/electron conducting polymers**

7
8 *Ariana Villarroel Marquez, Gerardo Salinas, Myriam Abarkan, Maël Idir, Cyril Brochon,*
9 *Georges Hadziioannou, Matthieu Raoux, Alexander Kuhn, Jochen Lang, Eric Cloutet**

10 **Chemicals**

11 4'-aminobenzo-18-crown-6; 4-styrene sulfonic acid sodium salt; 4-vinylbenzyl chloride;
12 azobisisobutyronitrile; oxalyl chloride; potassium carbonate; sodium carbonate; triethylamine
13 and all other products were used as received or according to manufacturer's instructions
14 (Sigma Aldrich, France). N,N-dimethylformamide (DMF) was distilled from calcium hydride
15 (CaH₂) prior to use. Acetonitrile was distilled prior to use or dried by a solvent dryer machine
16 (MB SPS-800, MBraun). Tetrahydrofurane was distilled from benzophenone/sodium prior to
17 use.

18 **Techniques and instrumentation**

19 *Nuclear magnetic resonance (NMR) spectroscopy:* ¹H-NMR and ¹³C-NMR spectra for
20 structural characterization and titration experiments were recorded on Bruker Avance
21 (300MHz) and Bruker Prodigy (400MHz) spectrometers, respectively, at 300K and the
22 residual proton signal of the solvent was used as the internal standard. *Size exclusion*
23 *chromatography (SEC)* was used to determine molar masses and dispersity of the copolymers
24 synthesized. The system (Agilent GPC220HT) is equipped with UV and RI detectors and is
25 equipped with a pre-column GF-1G-7B and two columns Asahipack GF-7MHSi (DMF, 0.1M
26 LiBr, T=75°C, flow rate=0.6mL/min). Polystyrene standards were used for calibration. *Film*
27 *Deposition:* A Brewer Science 200CBX spin-coater was used for film deposition. Substrates

1 were cleaned with a VWR ultrasonic cleaner. UV-ozone treatment was carried out using a
2 UVO cleaner 42A-220 from Jelight company inc. A Bruker Dektak XT-A profilometer was
3 used to measure film thickness.

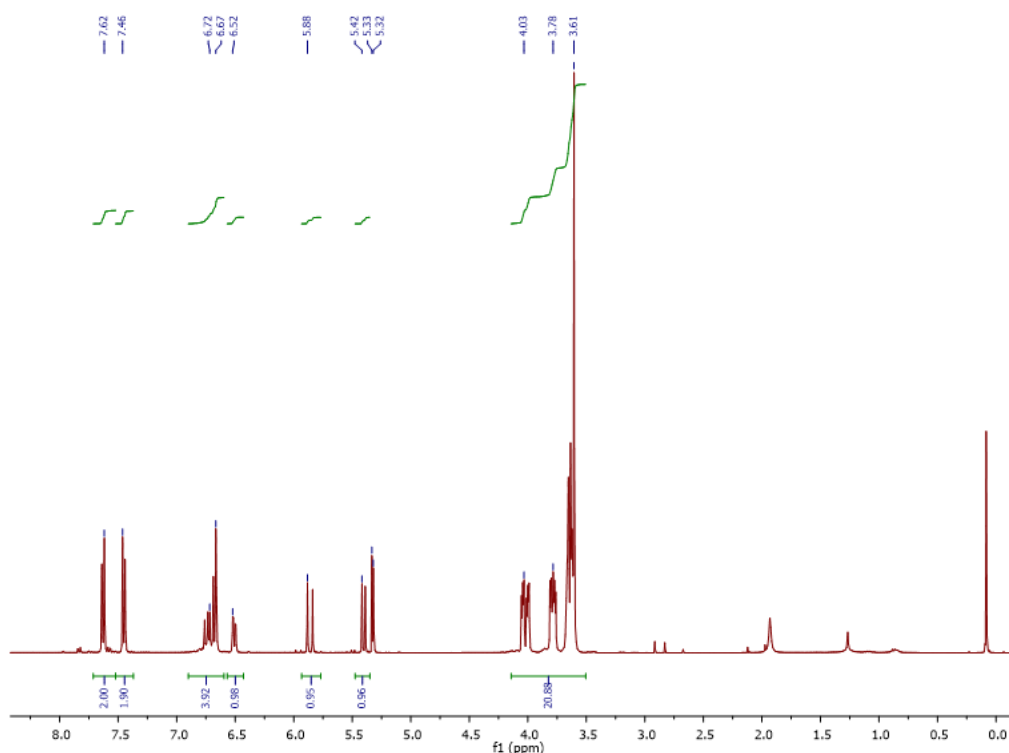
4 *NMR titrations:* Supramolecular titration experiments have been carried out at constant
5 concentration of the monomer under study (host) and increasing concentrations of the salt.
6 Spectra were recorded for every sample, observing the change in the chemical shift in the case
7 of $^1\text{H-NMR}$ spectroscopy. Variations in the chemical shift observed in $^1\text{H-NMR}$ spectroscopy
8 were fitted to a 1:1 binding model using Affinimeter^[1] software and from these data the global
9 association constants were extracted.

10 **Monomer synthesis and spectroscopy characterization**

11 *Step 1- Formation of 4-styrenesulfonyl chloride (1):* A round bottom flask, previously flame-
12 dried, was charged with dry and degassed acetonitrile (V=60 mL). Oxalyl chloride (5.91 g,
13 46.6 mmol, 1.2 eq.) and DMF were added. This solution was kept under stirring at room
14 temperature to solubilize the reagents and promote the Vilsmaier-Haack complex formation
15 for 4 or 5 hours. Once the characteristic yellow colour of the solution became stable, 4-
16 styrenesulfonic acid sodium salt (8.0 g, 38.8 mmol, 1.0 eq.) was added slowly to the solution
17 under nitrogen atmosphere and at room temperature. After 24h of reaction, the precipitated
18 salt was separated by filtration and the reaction mixture was used in the second step.

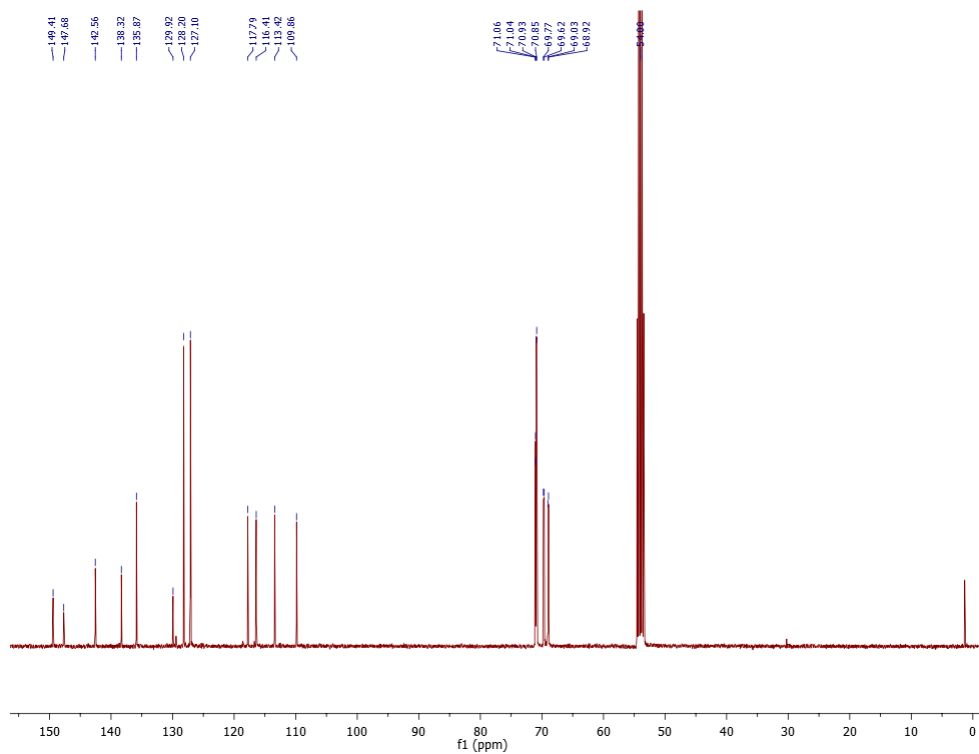
19 *Step 2- Synthesis of 4-styrenesulfonyl(phenyl-18-crown-6) imide (Sph18cr6SI) (2):* In a
20 second flame-dried round bottom flask containing dry and degassed acetonitrile (V=50 mL),
21 triethylamine (4.29 g, 30.2 mmol, 3 eq.) and 4'-aminobenzo-18-crown-6 (3.00 g, 10.1 mmol,
22 1 eq.) were added and stirred for one hour. During this time, the 4-styrenesulfonyl
23 chloride/acetonitrile solution (formed during Step 1) was cooled at 0 °C. Subsequently, the
24 trifluorosulfonamide solution was added in vacuum atmosphere to the former. Finally, the

1 mixture was allowed to warm up to room temperature and the reaction was kept running
2 under stirring for 16h. Purification was done firstly by removing under low pressure the
3 solvent mixture and solubilizing the monomer in dichloromethane. The product was obtained
4 by extraction with potassium carbonate and a subsequent wash with 1M hydrochloric acid
5 solution. Solvent was removed under low pressure and after drying overnight at 45°C under
6 vacuum, the product was recovered as a brown solid product. (yield=54%). Scheme 1. ^1H -
7 NMR (400 MHz; d-DMSO; 298K): $\delta(\text{ppm})= 7.79$ (d, 2H); 7.61 (d, 2H); 6.80 -6.52(q, s, dd,
8 4H); 5.99-5.94 (d, 1H); 5.48-5.36 (d, 1H); 3.98 – 3.50 (m, 20H). ^{13}C -NMR (75 MHz; d-
9 DMSO; 298K): $\delta(\text{ppm})= 147.9$; 145.46; 141.1; 138.4; 135.2; 130.54; 127.9; 127.15; 126.84;
10 126.63; 117.76; 113.93; 113.14; 107.7; 68.82; 69.74-67.97. m/z (ESI-HRMS) 516.17 ([MNa⁺]
11 $\text{C}_{24}\text{H}_{31}\text{NO}_8\text{SNa}$ requires 516.57).



12

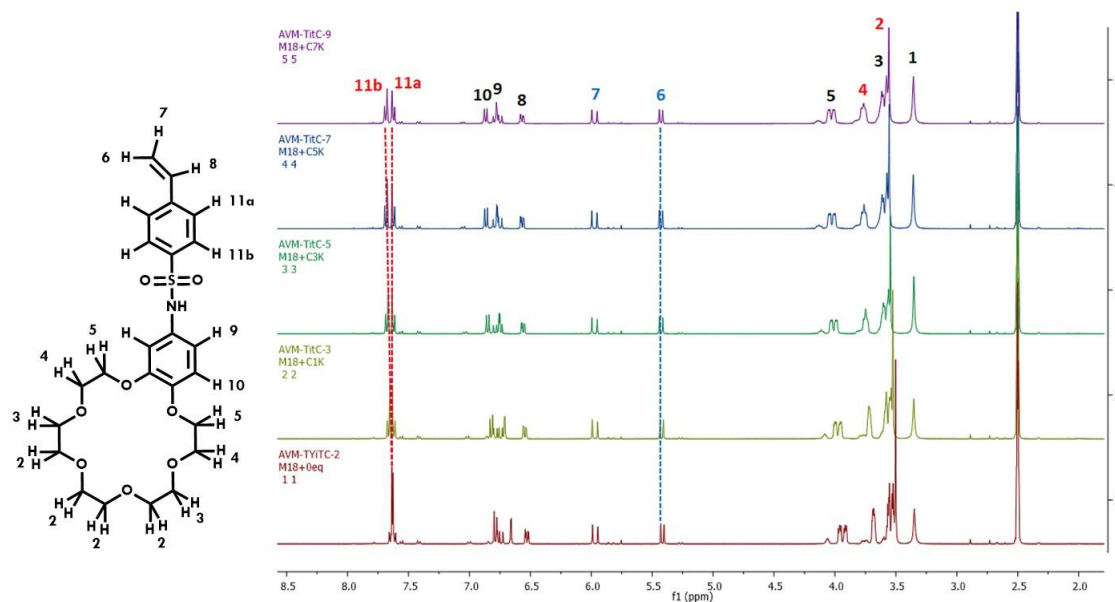
13 **SI-1.** ^1H -NMR (CD_2Cl_2 , 400 MHz) of 4-styrenesulfonyl(phenyl-18-crown-6) imide (2).



1

2 **SI-2.** ^{13}C -NMR (CD_2Cl_2 , 150 MHz) of 4-styrenesulfonyl(phenyl-18-crown-6) imide (2)

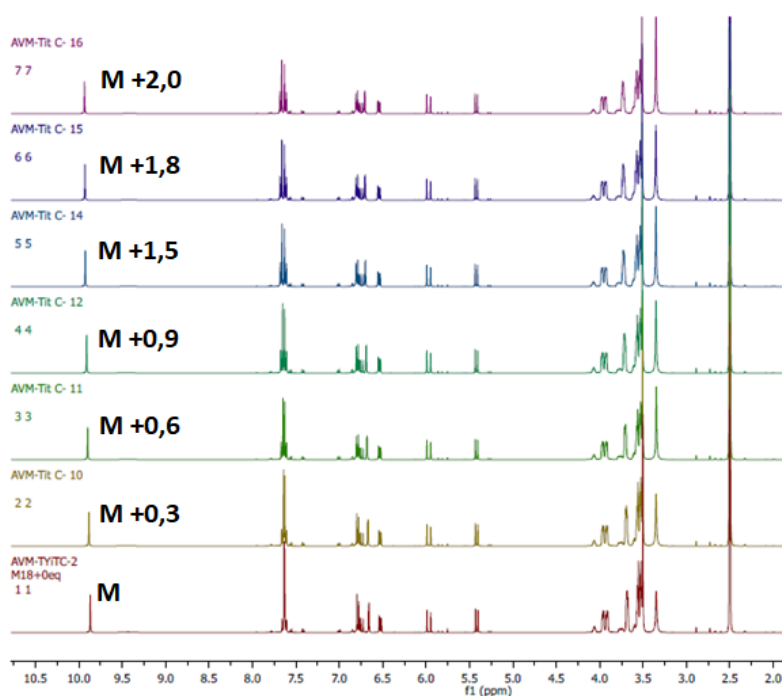
3 *Binding ability evaluation by ^1H -NMR titration of monomer (2)*



4

5 **SI-3.** ^1H -NMR Spectrum (DMSO, 400 MHz) obtained for the titration of the monomer (2)

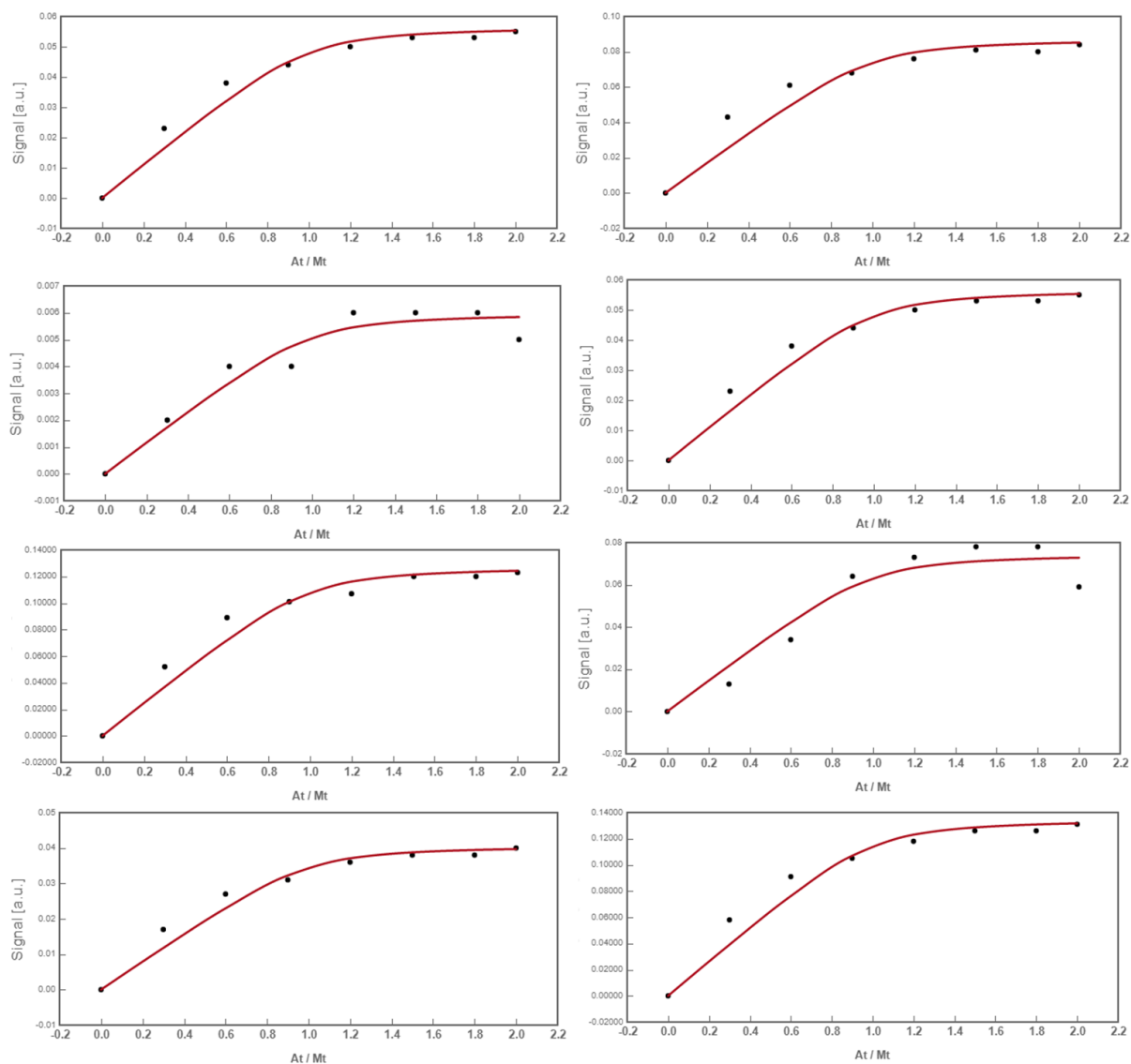
6 under variable concentrations (from 0 to 2 molar equivalents) of potassium perchlorate.



1

2 **SI-4.** $^1\text{H-NMR}$ Spectrum (DMSO, 400 MHz) obtained for the titration of the monomer (2)

3 under variable concentrations (from 0 to 2 molar equivalents) of sodium perchlorate.



1

2 **SI-5.** Binding isotherms and fitting to a 1:1 binding model of the experimental data from ^1H -

3 NMR titration of the monomer (2) (d-DMSO, 400 MHz). Scattered dots: Experimental data

4 obtained from the difference in NMR shift (ppm) with respect to initial monomer spectra (y-

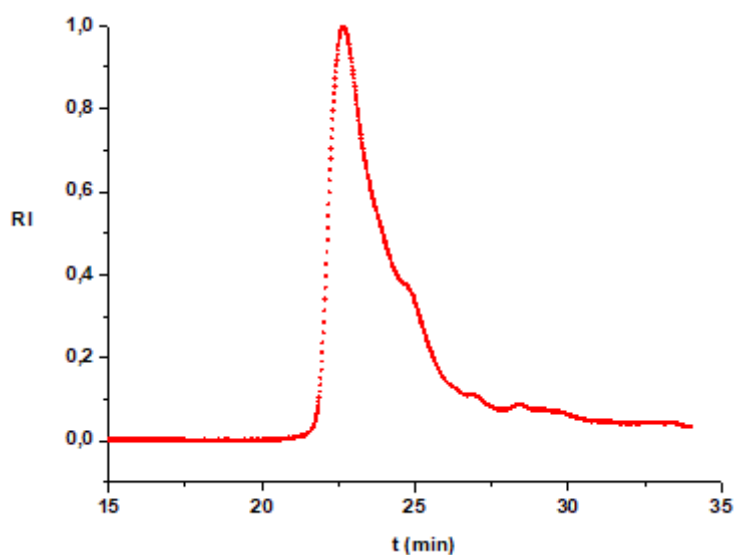
5 axis – “Signal”) vs the increasing concentration of KClO_4 , for a constant monomer

6 concentration, Mt (x-axis – “At/ Mt”). Red curves: Fitting to the different binding isotherms

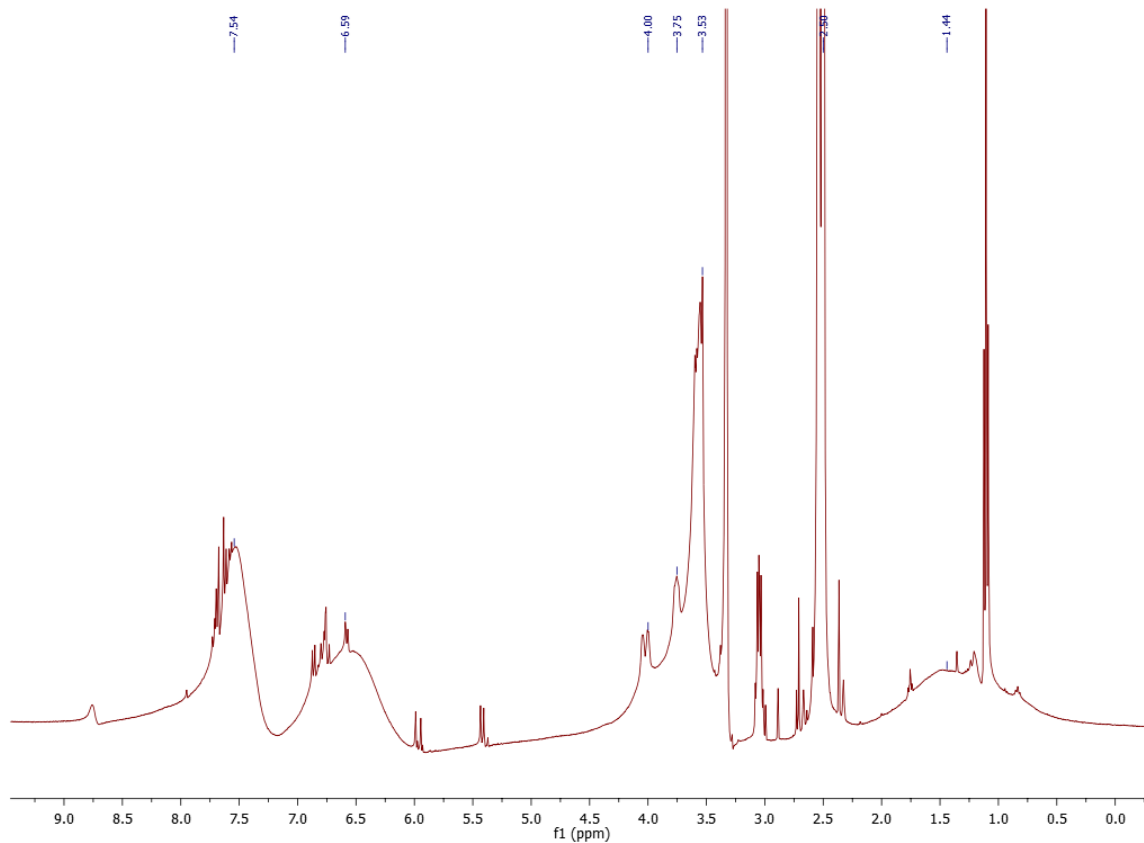
7 with a 1:1 binding model to obtain the global binding constant (K_A).

8

1 *Radical polymerization and Copolymerization (GENERAL PROCEDURE):* The copolymers
2 between STFSI monomer and ion-sensitive styrene monomer (2) were synthesized by
3 reversible addition-fragmentation chain-transfer (RAFT) radical polymerization by mixing,
4 according to the targeted molar mass and composition, the proper quantity of the STFSI/(2)
5 monomers, chain transfer agent and azobisisobutyronitrile (AIBN) in DMF. After several
6 freeze-thaw cycles, the mixture was left to polymerize at 64°C from several hours to few
7 weeks, depending on the molar mass that should be obtained. The polymer was ready after
8 precipitation in tetrahydrofuran (THF) or the adequate solvent mixture, filtration, washing
9 with THF and drying in vacuum oven at 65°C for at least one day.



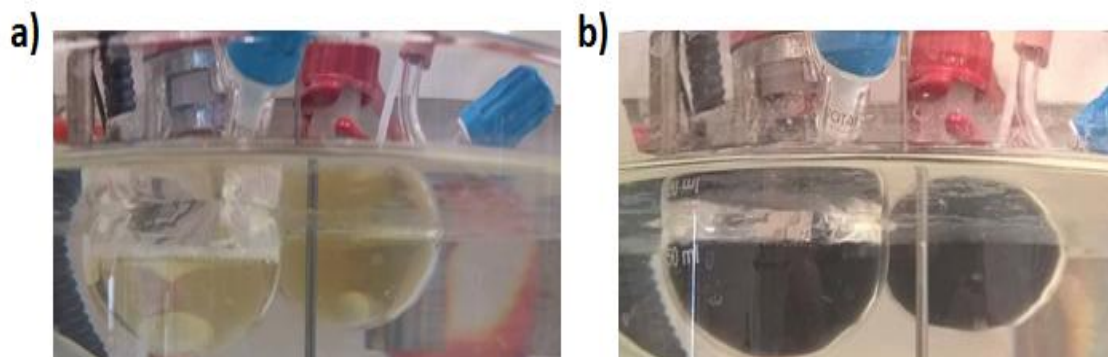
11 **SI-6.** Size exclusion chromatogram (SEC) of a copolymer between STFSI (wt.% = 85) and
12 monomer (2) (wt.% = 15) showing a main population of 135 kDa. Conditions: Polystyrene
13 standard calibration. DMF, LiBr, 70°C.



1
2 **SI-7.** $^1\text{H-NMR}$ Spectrum ($\text{d}_6\text{-DMSO}$, 400 MHz) of a copolymer between STFSI (wt.% = 85)
3 and monomer (2) (wt.% = 15).

4 *Conductive ion sensitive aqueous PEDOT dispersions:* Solutions of iron chloride (III) (0.036
5 mg, 0.22 mmol), ammonium persulfate (0.161 g, 0.71 mmol) and the styrene-based
6 copolymer (0.210 g) were prepared in individual aqueous solutions and stirred during 5h
7 previous to their use. Afterwards, the polyelectrolyte solution was transferred to the reactor
8 and EDOT monomer was added (0.038 mL, 0.36 mmol) keeping under nitrogen flow at 10°C
9 for 30 min. Addition of the oxidant solutions composed of iron chloride and ammonium
10 persulfate starts the polymerization. The reaction is kept running under static inert atmosphere
11 during 64h. Purification has been done by ultrafiltration, washing firstly with 1M
12 hydrochloric acid (150mL). After stirring for two more hours with a 50% content of the
13 previous used acid solution, a last washing with water was performed. Concentrations were
14 adjusted to about 1 weight % of content after filtration, in correlation with a calibration curve

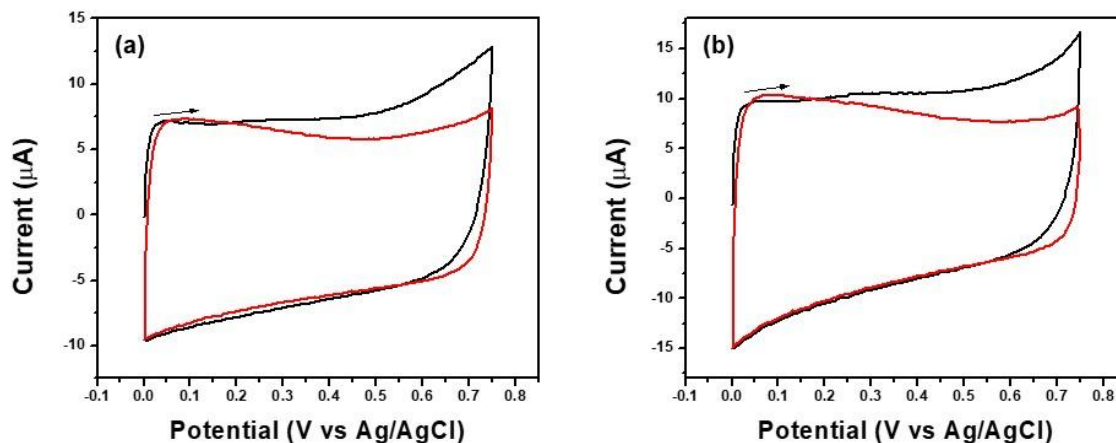
1 obtained by UV-Vis absorption spectroscopy analysis. Inks were stored protected from light
2 at constant temperature and under stirring.



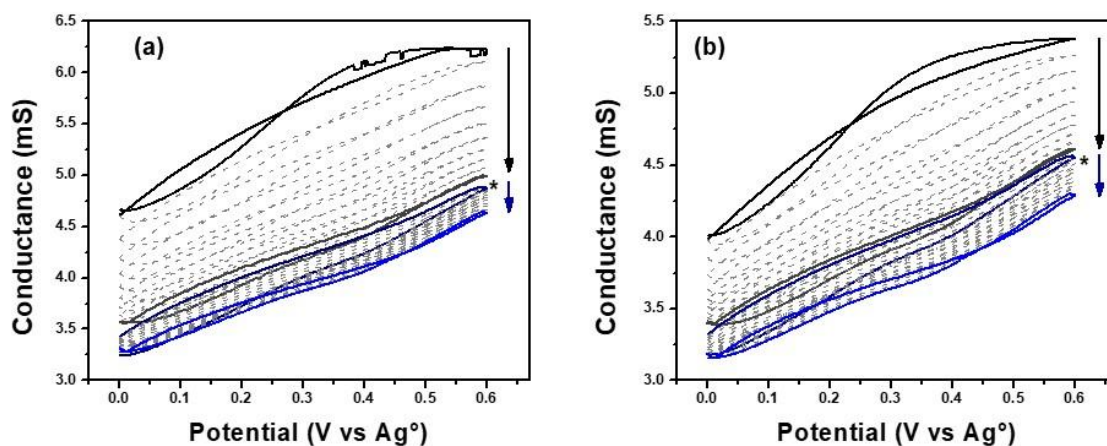
3
4 **SI-8.** Aqueous dispersion formation of the ion-sensitive PEDOT based ink: a) Before the
5 addition of the oxidants, brownish polyelectrolyte solution; b) After addition of the oxidants,
6 formation of the PEDOT based ink.

7 *In-situ electrochemical-conductance measurements:* *In-situ* electrochemical-conductance
8 measurements were carried out using a two potentiostat system, specially built for this
9 application. As working electrodes, DropSens interdigital microarrange electrodes (IDMAE),
10 featuring separated Pt bands (10 μm) deposited on it, were used. A three-electrode
11 electrochemical cell fitted with a Pt foil counter electrode separated approximately 0.5 cm from
12 the working electrode (parallel and of the same size as the working electrode), a pseudo-
13 reference electrode (Ag wire) and the IDMAE were used for the studies. A constant potential
14 difference of 10 mV provided by one potentiostat was applied between the IDMAE branches
15 to generate the drain current that circulates through the polymer during conductance
16 determinations. The conductance of the dropcasted films was measured in real time during the
17 cyclic voltammetry experiment in an aqueous 0.1 M tetramethyl ammonium chloride
18 (TMAC) solution at 25 °C. Conductance was calculated according to Ohm's Law, which is
19 directly related with specific conductivity. More details about this technique and examples of

1 the use of conductance measurements in conducting polymers can be found elsewhere in the
 2 literature^[2]

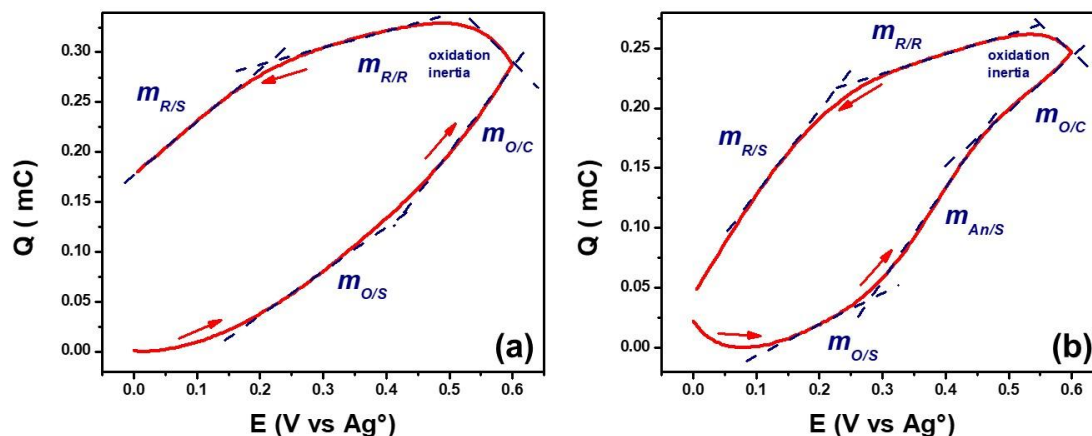


3
 4 **SI-9.** Potentiodynamic response of PEDOT electropolymerized in the presence of (a) PSS and
 5 (b) PSTFSI, in a free monomer 0.1 M PSS aqueous solution, $\nu = 50 \text{ mV/s}$, 1st cycle (black
 6 line) and 10th cycle (red line).



7
 8 **SI-10.** Conductance profile of drop casted PEDOT/ P(STFSI85-co-S18cr615) films in a 0.1 M
 9 TMAC aqueous solution using $E_{\lambda} = 0.6 \text{ V vs Ag}^{\circ}$, $\nu = 10 \text{ mV s}^{-1}$ and ΔV on the WE = 10 mV,
 10 WE = Pt IDMAE, CE = Pt foil, in the absence (initial 10 cycles) and the presence of (a) 10
 11 mM KCl and (c) 10 mM NaCl (final 10 cycles). The asterisk indicates the moment when
 12 addition of the chloride salts was performed.

1



2

3 **SI-11.** Charge-potential plots of a drop-casted film in a 0.1 M TMAC aqueous solution
 4 obtained from the integration of the (a) 1st and (b) 10th potentiodynamic scan.

5 *Cytotoxicity evaluation: direct evaluation and apoptosis test:* Determination of the rate of
 6 programmed cell death was performed by the use of a LIVE/DEAD Kit (ThermoFisher
 7 Scientific, USA). This sensitive two-colour fluorescence cell viability assay allows
 8 discrimination between alive and dead cells with two probes that measure established
 9 parameters of cytotoxicity and cell viability, i.e. intracellular esterase activity and plasma
 10 membrane integrity. Polymer films were deposited on coverslips (18 mm diameter). Prior to
 11 use, they were washed (by sonication in acetone, ethanol and isopropanol baths), air dried and
 12 activated (surface plasma cleaning, 15min). Films were formed by spin-coating of the ink
 13 (previously formulated) at the optimal speed to obtain maximal film coverage (generally for
 14 30 s at 500-800 rpm, followed by a cycle at 1200-1800 rpm). Coated coverslips were cured at
 15 50°C for 10 min followed by heating to 120°C for one hour. After cooling, films were placed
 16 in a 12 well multiwell that had been sterilized by UV treatment ($\lambda=254$ nm, 30 min) prior to
 17 cell culture. Before adding cells in the medium, coverslips were rinsed with 1.5 ml/well of
 18 PBS^{+/+} buffer (composition in mM: KCl 2.67; KH₂PO₄ 1.67; NaCl 138, Na₂PO₄ 8, CaCl₂ 1.8,

1 MgCl₂ 1.0) and dried overnight. 50,000 INS-1 clonal β -cells were added per well and cultured
2 as described for 3 days.^[3] Coverslips were either visualized and documented by phase contrast
3 microscopy or further processed for apoptosis measurements. In the latter case, cell media
4 were replaced by fresh media with or without thapsigargin (0.1 μ M, as positive control) for 6h
5 prior to analysis. Imaging was used after de-freeze. The Live/Dead cell kit was used
6 according to the manufacturer and 150 μ L of final solution were added per coverslip for 15
7 min at 37°C followed by imaging. For each data point three coverslips were examined,
8 experiments were repeated independently nine times and areas of fluorescence calculated by
9 ImageJ.^[4] Statistical analysis was performed using GraphPad Prism7.

10 **References**

11 [1] Data fitting was performed with the AFFINImeter server (<http://www.affinimeter.com>).
12 Unless stated otherwise the experimental data were fitted using a simple 1:1 binding model.

13 [2] G. Salinas, B. A. Frontana-Uribe, *ChemElectroChem* **2019**, *6*, 4105.

14 [3] B. Hastoy, P. A. Scotti, A. Milochau, Z. Fezoua-Boubegtiten, J. Rodas, R. Megret,
15 *Scientific Reports* **2017**, *7*, 2835.

16 [4] ImageJ2: ImageJ for the next generation of scientific image data", *BMC Bioinformatics*
17 *18*, 529,

18